

CHARACTERIZATION OF SORPTION BEHAVIOR AND MASS TRANSFER PROPERTIES OF FOUR CENTRAL AFRICA TROPICAL WOODS: AYOUS, SAPELE, FRAKE, LOTOFA

Merlin Simo-Tagne^{1,}, Romain Rémond², Yann Rogeume², André Zoulalian³, Patrick Perré⁴*

ABSTRACT

This study provides the sorption isotherm, its hysteresis and their mass transfer properties of four Central Africa Tropical woods widely used for building construction: frake (*Terminalia Superba*), lotofa (*Sterculia Rhinopetala*), sapele (*Entandrophragma Cylindricum*) and ayous (*Triplochiton Scleroxylon*). Characterization of these four species in particular and Central Africa tropical woods in general were necessary to develop conservation and treatment of wood after first transformation using the drying. Also, moisture transport on wooden material used such as wall buildings can be facilitating to found the thermal comfort. Measurements of isotherms were performed using a dynamic vapor sorption apparatus (*Surface Measurement Systems*) at 20 and 40°C with air relative humidity ranged from 0% to 90%. Mass diffusivity was determined in steady state using a specific vaporimeter. Air permeability was determined using a specialized device developed to measure over a wide range of permeability values. Permeability and mass transfer properties were determined in the tangential direction with a "false" quartersawn board (sapele and lotofa) and in the radial direction with a flatsawn board (ayous and frake). Samples of sapele, ayous and frake are heartwood when lotofa contains as well as heartwood than sapwood. Results obtained showed that the temperature effect on sorption behavior was quite low. We observed also a low difference between the sorption behavior of these different species and hysteresis of sorption decreases when temperature increases. Hailwood-Horrobin model's explains plausibly the experimental sorption isotherms data. Results on characterization of mass transfer properties showed that, in the steady state, mass diffusivity decreases exponentially when basal density increases. Mass diffusivity was higher in desorption than in adsorption phase. The gaseous permeability of these species was between than those of Australian hardwoods and temperate woods. It was difficult to define a relationship between permeability and mass diffusivity.

Keywords: Air permeability, Central Africa, diffusion coefficient, sorption isotherm, tropical woods.

¹Higher Teacher Training College, Applied Physic Laboratory, Yaoundé, Cameroon.

²University of Lorraine, LERMAB, ENSTIB, Epinal, France.

³University of Lorraine, LERMAB, Faculty of Sciences and Techniques - Aiguillettes Campus- Nancy, France.

⁴Ecole Centrale de Paris, LGPM, Châtenay-Malabry, Paris, France.

*Corresponding author: simotagne2002@yahoo.fr

Received: 23.02.2015 Accepted: 06.12.2015

INTRODUCTION

Tropical woods have economic and ecological importance, and it is important to optimize the exploitation of tropical forests. For example, Cameroonian forests have more than 300 wood species but only three species (sapele, ayous and azobe) represent almost 70% of the total production. In 2001, the volume ratio of rough timber of ayous exported from Cameroon represented almost 51% (ATIBT 2002). Cameroon and Gabon have voted the laws which impose the first transformations of their tree species in each country. However, few transfer properties of Central Africa wood species have already been studied in the literature. Agoua (2001) and Zohoun *et al.* (2003) studied the mass diffusivity of the teck (*Tectona grandis*) from the southern Benin. Kouchade (2004) studied the mass diffusivity of doussie, movingui and ayous species. A good knowledge of the thermophysical properties of wood can help to efficiently use the woods and achieve maximum values. Additionally, a better knowledge of the material properties of these species is required to improve on their drying and propose new drying schedules, some conditions of preservation and moisture transport on wood and wooden material. That allows using in some numerical models developed in literature to predict the timber drying (Pang 2007, Perré 2004, Perré and Turner 1999, Simo *et al.* 2010, Simo *et al.* 2011, Turner and Perré 1995). In the building domain with wall made in wood, these parameters are most important to predict interior air quality, acoustic and thermal comfort, energetic bill and conservation of the frame.

The main objective of this paper is to provide a better knowledge of the mass transfers' properties of these tropical species. Characterization experiments are achieved in this work to provide: (1) their sorption isotherms, (2) the mass diffusion coefficients which define the mass flux in response to a concentration gradient, and (3) the gas (air) permeability which defines the mass flux in response to a pressure gradient.

The present work is performed on frake (*Terminalia Superba*), lotofa (*Sterculia Rhinopetala*), sapele (*Entandrophragma Cylindricum*) and ayous (*Triplochiton Scleroxylon*). The four wood species for this experiment were classified into medium and low density using the classification taken from Benoit (2008). The classification showed frake and ayous as low density wood, lotofa and sapele as medium density wood. These wood species came from Cameroonian forests. Before presenting and discussing our obtained results, we remind briefly the experimental methodology employed to reach the studied thermophysical parameters.

MATERIALS AND METHODS

All tests presented here have been done in the Studies and Research on Wood Material Laboratory (LERMAB) of University of Lorraine, localized in Epinal, France.

Material sampling

Specimens were collected from natural forests of Douala Cameroon and were prepared in the LERMAB. Basic densities of these samples taken from Simo (2014) are close to the average value given from the FCBA's and Cirad's data (Benoit 2008). Board with dimensions 426x75x13mm was prepared and dried until moisture content reached 10% with an air relative humidity of 80% and a dry temperature of 65°C. Circular disks, as shown in Figure 1, with a diameter close to 73 mm and with thickness in the diffusion transfer direction close to 13mm were cut from these boards (Table 1). These specimens were used to determine both the mass diffusion coefficient and air permeability. However, despite the care taken at the time of sampling, the annual ring orientations; viewed from the end, have a relative angle between the rings and the surface that changes along the thickness and also along the board's length. Additionally, lotofa's samples are a mixture between heartwood and sapwood and the samples of the other species are essentially constituted by the heartwood. The specimens used

to determine the sorption isotherms were very fine wood-chips cut with a microtome blade to obtain samples on each board with dimensions approximately 1x0,5x2mm (Figure 1).

Table 1. Geometrical characteristics of the studied samples.

| Tests | Specimen type | Specimen number | Specimen size in mm |
|--------------------|---------------|--|---------------------|
| Mass diffusivity | Disk | 4 by species | Diameter 73 |
| Air permeability | | | Thickness 13 |
| Sorption isotherms | Fiber | Some fibers with 10mg approximately by species | 1x0,5x2 |

Sampling collection is summarized in table 1. We have repeated each experiment on each specimen for confirmation. Thus, eight experiments have been done on each species. Comstock and Côté (1968) had used two or more specimens and average values were presented. Kouchade (2004) had determined the mass diffusion coefficients of African tropical woods using indirect method from electrical resistant measurements in unsteady state with thickness equal to 5mm reported according to radial and tangential directions in desorption and adsorption phase. He had used two to five specimens by species and orthotropic direction and average value is recorded. It is the first time to characterize the studied woods using described tests.

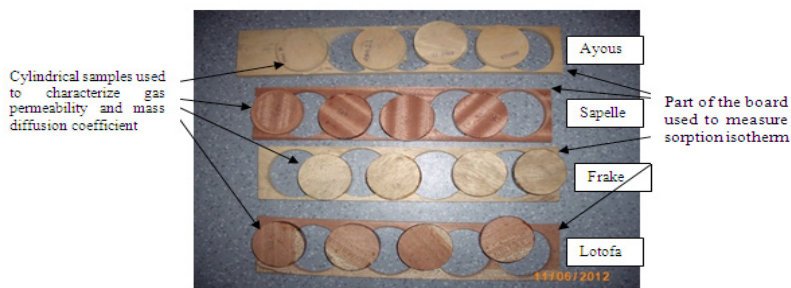


Figure1. Wood samples used in this study and extraction of cylindrical forms.

Experimental device to determine mass diffusion coefficients

We have used an experimental set-up presented in figure 2. This set-up is formed by four principal elements: a computer, a cryostat, a climatic chamber and an electronic balance. The cryostat permits to regulate the temperature in the climatic chamber. The computer is used to record air relative humidity and air temperature during the experiment. In the climatic chamber, the electronic balance permits to weigh the mass adsorbed or desorbed by the sample at a chosen time intervals during the experiment. The climatic chamber used in this study was developed in the laboratory of ENGREF. The relative humidity is controlled through the temperature of a water film that flows at the bottom of the chamber, and electrical resistances heat the air flow at the top of the chamber. Two centrifugal fans and a water pump provide homogeneous conditions within the chamber. The drying parameters are maintained by a double loop PID controller connected to a personal computer. In the climatic chamber, air relative humidity is evaluated to 59% during the experiment. Figure 2 shows the climatic chamber and a detailed description of this device is given by Zohoun *et al.* (2003), Agoua *et al.* (2001) and Rousset (1999).

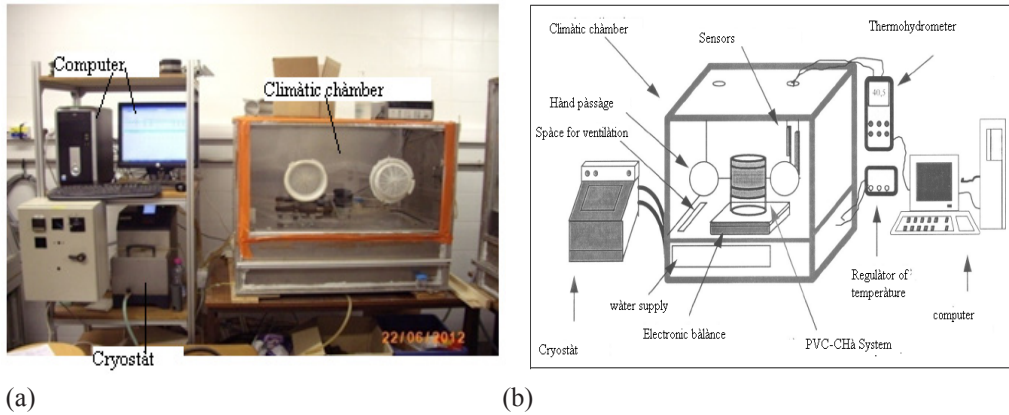


Figure 2. Equipment to measure mass diffusion coefficient in the permanent phase (a) Picture; (b) Schematic illustration of the basic principle (Rousset 1999).

Sorption analyzer

Isotherms were performed using a dynamic gravimetric water sorption analyzer (Figure 3) from Surface Measurement Systems (DVS-Intrinsic). Comparing by traditional method where several months are necessary to obtain equilibrium state, this method permits to obtain equilibrium state in the short time in the range 0-95% RH. The sample was weighted using a digital microbalance (total capacity of 1 g; noise < 1 μ g). For this test, each sample had an initial mass of approximately 10 mg. The sorption cycles applied in this work started from zero percent relative humidity (RH) and the temperatures were 20°C and 40°C, respectively. Samples were maintained at a constant RH level until the weight change per minute (dm/dt) value reached 0,0005% per minute (Figure 4). This rate value is more severe than that used in previous works. For example, Hill *et al.* (2009) fixed a dm/dt of 0,002% per minute and attested that using this value permits to obtain a sample moisture content within less that 0,1% of the equilibrium value at extended time.

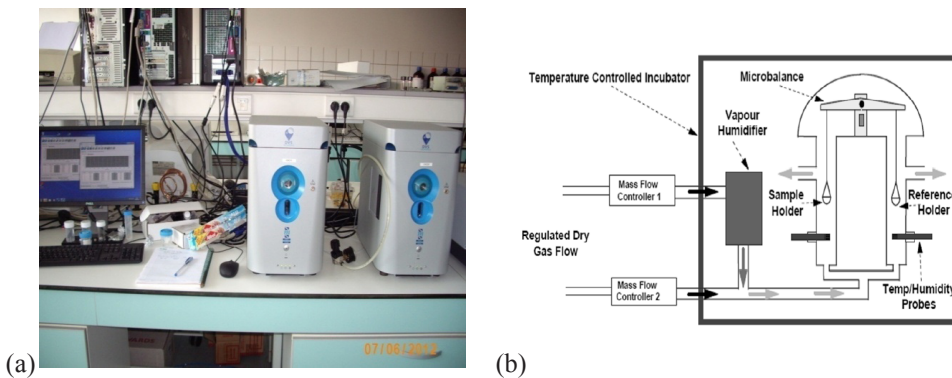


Figure 3. DVS apparatus used to measure different sorption isotherms.(a) Picture; (b) Schematic illustration of the basic principle (Engelund *et al.* 2010).

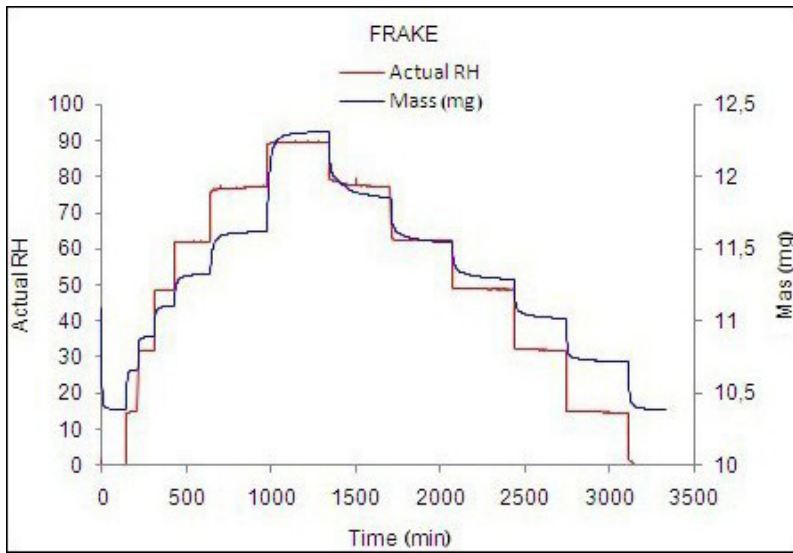


Figure 4. Mass and relative humidity of the fiber of frake during sorption isotherms determination.

The raw DVS data was first analyzed using the DVS Standard Analysis System. This software permits construction of sorption isotherms and hysteresis curves. For all samples, equilibrium moisture content values were determined using the last fifteen data of each plateau. For a more detailed description of DVS System, see Surface Measurement Systems (2015).

Applying Hailwood-Horrobin (HH) model on envelope curves

The HH model (eq.1) (Hailwood-Horrobin 1946) is most used since 1970s to describe the sorption isotherms of wood (Mantanis and Papadopoulos 2010, Olek *et al.* 2013, Simpson 1973, Simpson 1980).

The simplified equation of this model is used in this work to describe the envelope curves (air relative humidity ranged from 0% to 90%). The HH sorption model is based on the assumption that the sorbed water exists as a simple solution and as hydrate of the wood. The HH-model assumes further that the sorbed layer which consists of no hydrated, hydrated wood and of free liquid water forms an ideal solid solution (Popper *et al.* 2009). The measured sorption isotherm is plotted as RH/X against RH as it was proposed in several works such as Time (1998). The obtained parabola is then fitted to the plotted points and the values of the empirical constants A, B and C are calculated using linear regression techniques.

$$X = \frac{RH_b}{A + B.RH_b - C.RH_b^2} \quad (1)$$

With: b=Ad for adsorption and b=De for desorption curves. RH is the relative humidity (-), X is the equilibrium moisture content (kg of water/kg of oven-dry material). A, B and C are the shape factors.

Mass diffusion coefficient measurement The cup method

The water vapor diffusivity of wood samples was measured under the steady-state condition (Agoua *et al.* 2001). The vaporimeters are used in these experiments and are based on the PVC-CHA system. Several cups were filled with a NaCl solution for desorption phase, providing a RH of 75% (at 33,5°C) (detail in Figure 5 and 6). Agoua *et al.* (2001), Mouchot *et al.* (2006) and Rousset *et al.* (2004) give more details about this device. In the case of adsorption phase, Silica gel solution is used providing a RH of 0% at 33,5°C. The cups with attached 13 mm-thick samples were then placed in a conditioning chamber (RH=59%, T=33,5°C). The cups were weighed two times by day when a constant slope was reached. After 10 days, when a steady-state condition was reached, the cup weight loss (and gain) was plotted in function of the time. In fact, the steady-state condition was determined by the daily measurements of the cup weight.

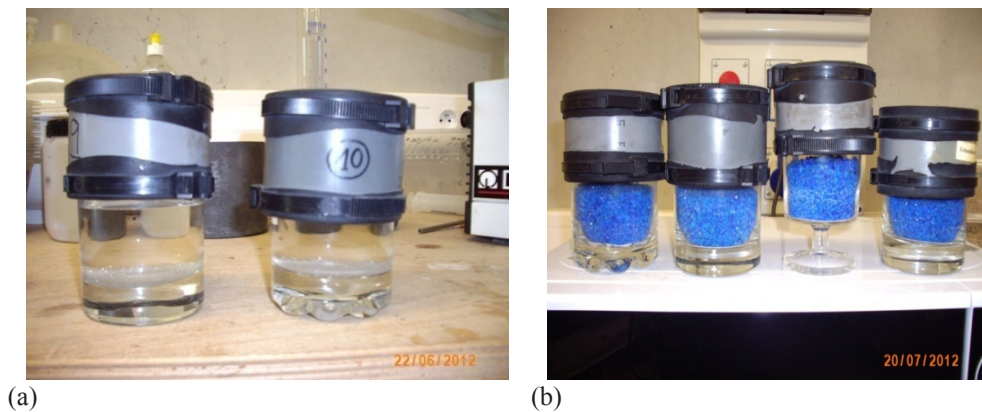


Figure 5. PVC-CHA system for determination of mass coefficient diffusion (vaporimeter)(a) PVC-CHA with NaCl (weight loss sequence) (b) PVC-CHA with silica gel (weight gain sequence).

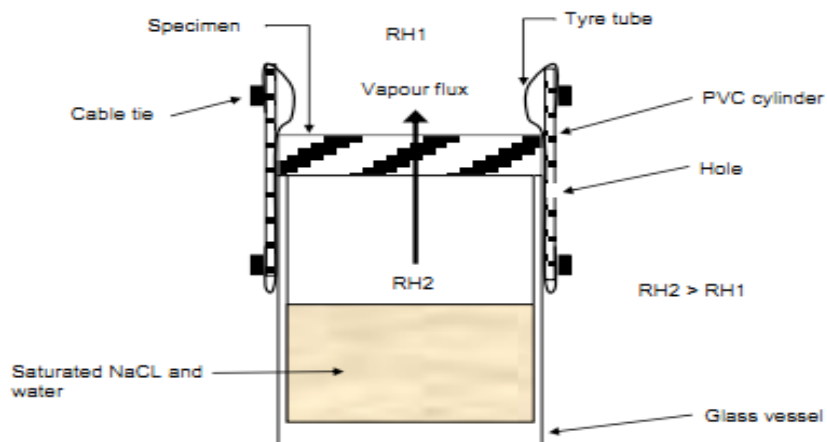


Figure 6. Annotation of PVC-CHA system, in the weight loss sequence (Redman *et al.* 2012).

Identification of the mass diffusion coefficient

The water vapor flux through the wood sample ($\text{kg}\cdot\text{s}^{-1}\cdot\text{m}^{-2}$) was calculated from equation 2a (Agoua *et al.* 2001).

$$q = -f D_v \nabla(\rho_v) \quad (2a)$$

Where f is dimensionless diffusion coefficient through the wood samples, ρ_v is water vapor density ($\text{kg}\cdot\text{m}^{-3}$). D_v is the binary diffusion coefficient of vapor in air (m^2/s) and is expressed by equation 2b.

$$D_v = 2,26 \times 10^{-5} (T / 273)^{1,81} \times P_{atm} / P \quad (2b)$$

T is the air temperature (K) and P the air pressure (Pa).

In the case of steady state, the dimensionless diffusivity, defined by the ratio between the vapour diffusion into the product and the diffusivity of water vapour in air, is introduced by Agoua *et al.* (2001) and is experimentally expressed as follow (Gholamiyan *et al.* 2012) :

$$f_{exp} = \frac{Q \ell R T}{D_v S |RH_1 - RH_2| P_{vs}(T) M_v} \quad (2c)$$

Where Q is the measured mass flow ($\text{kg}\cdot\text{s}^{-1}$) represented by the slope of gain mass(kg) versus time (s) for adsorption phase, or the slope of loss mass (kg) versus time (s) for desorption phase, S the transversal section of the sample (m^2), M_v the molar mass of vapour ($\text{kg}\cdot\text{mol}^{-1}$), RH the relative humidity (-), T the temperature (K), R the ideal gas constant ($\text{J}\cdot\text{mol}^{-1}\cdot\text{K}^{-1}$), ℓ the thickness of the sample (m), P_{vs} the saturated vapour pressure (Pa). $| |$ is the absolute value symbol.

A correction of the f_{exp} value has been taken in order to integrate the mass transfer resistance of the air volume included between the sample and the salt solution. The corrected dimensionless diffusivity can be obtained with the following expression (Zohoun *et al.* 2003):

$$f_{corrected} = \frac{1}{\frac{1}{f_{exp}} - \frac{e_a}{\ell}} \quad (3)$$

Where e_a is the distance between sample and salt solution, ℓ the sample thickness. Thus, mass diffusion coefficient is given by Zohoun *et al.* (2003) and is expressed as follow:

$$D = \frac{f_{corr} D_v M_v}{\rho_H R T} \frac{|P_{v_2} - P_{v_1}|}{|x_2 - x_1|} \quad (4)$$

ρ_H is the density ($\text{kg}\cdot\text{m}^{-3}$) of specimen studied equilibrium state. Simo (2014) has experimentally obtained (in kg/m^3) 471,8; 741,4; 456,2 and 791,9 for ayous, sapele, frake and lotofa respectively. $|x_2 - x_1|$ and $|p_{v2} - p_{v1}|$ are absolute values of the differences of equilibrium water content and vapor of pressure respectively between inside and outside positions of the PVC-CHA. When NaCl solution is used, air relative humidity in each cup (75%) is higher than air relative humidity in the climatic chamber (59%) and during experiments, the vapor passed from the cup to climatic chamber and loss mass is observed. When silica gel is used, air relative humidity in each cup (0%) is lower than the one in the climatic chamber (59%) and during experiments, the vapor passed from the climatic chamber to the cup and gain mass is observed.

Gas permeability measurement

The system Alu-Cha developed in Agoua (2001) and presented in figure 7a is capable to measure the air permeability through the sample. A constant air pressure difference is applied between the two faces of the sample. A mass flow meter estimates the gas flux passing through the sample. In order to ensure air tightness, a pressure of 0,2 MPa press a rubber joint against the lateral faces of the sample during the measurement. The air permeability is calculated using Darcy’s law (equation 5) such as in Comstock and Côté (1968). Thus, the measurement was carried out by applying a controlled and constant pressure difference (ΔP) between two faces of the specimen and then measuring the corresponding air flux (Q_L)

$$K = \frac{Q_L \mu e P}{PS \Delta P} \quad (5)$$

K the intrinsic permeability (m^2), Q_L the air flux (m^3/s), μ the dynamic viscosity of air ($\text{Pa}\cdot\text{s}$), e the sample thickness (m), DP the pressure difference between the sample faces, P the averaged pressure (Pa).

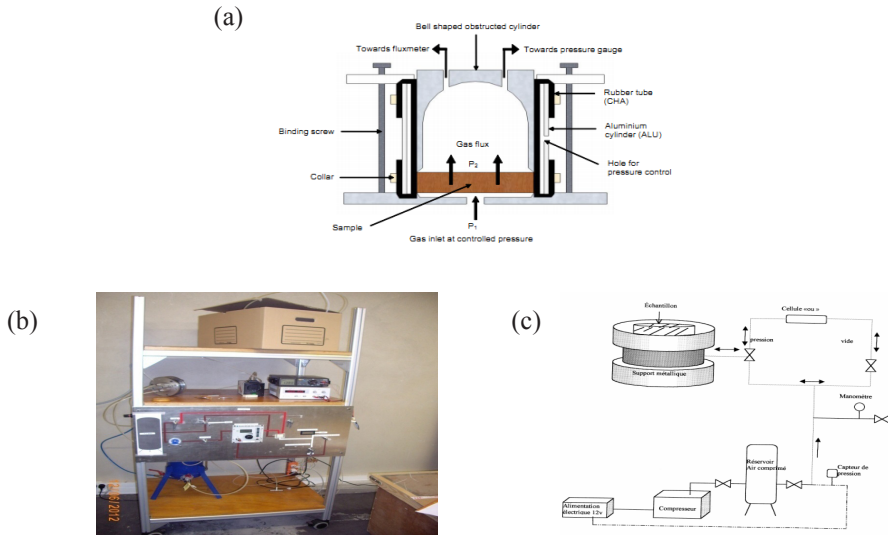


Figure 7. The system Alu-Cha and circuit to measure gas permeability. (a) Support Alu-Cha with the sample (Redman *et al.* 2012), (b) Apparatus of the measure gaz permeability parameter, (c) Circuit to take pressure (Agoua 2001)

Gas permeability was performed using a circuit presented in Figure 7b and 7c. Plotting DP versus Q_L , we must obtain a straight line passing through the origin whose slope allows estimating K using equation 5. Typically, four or five points of constant pressure difference are taken between 50 and 1000 mbar.

RESULTS AND DISCUSSION

Isotherms of sorption

The experimental sorption isotherms of the studied species are presented in the Figure 8 through 11. They present a sigmoid form which is characterized by a combination of hydrated water (monolayer of water molecules) and dissolved water (multilayer of water molecules). The shape of sorption isotherm curves is typical for wood as it was also observed by Alix *et al.* (2009), Englund *et al.* (2010), Fernández *et al.* (2014), Jalaludin *et al.* (2009), Jannot (2008), Schmid and Naderi (2010) and Tekleyohannes (1995). At a given air relative humidity, when temperature increases, equilibrium water content decreases. The effect of the temperature on the sorption isotherms is quite low. The results also conform to those of Björk and Rasmuson (1995) obtained at 140°C and 160°C. But the sorption isotherms presented in the literature and obtained on some tropical woods indicate a slightly higher effect of temperature (Beguide and Simo 2005, Jannot *et al.* 2006). According to Time (1998) and Björk and Rasmuson (1995), the contents of extractive, cellulose, hemicelluloses and lignin of studied woods are different than those of tropical woods studied in the literature and cited above. At a given relative humidity, equilibrium moisture content is higher during desorption than adsorption phase. The sorption hysteresis of studies woods get closer when air temperature increases, the maximum value is reached at a relative humidity of 60% (Figure 12).

: frake, lotofa, sapele and ayous.

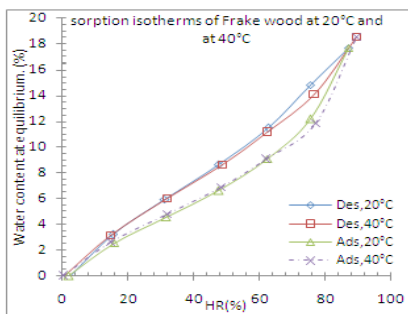


Figure 8: Sorption isotherms of frake (*Terminalia superba*)

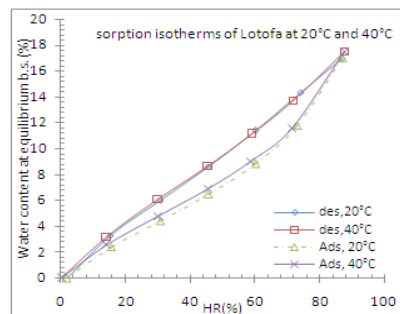


Figure 9: Sorption isotherms of lotofa (*Sterculia rhinopetala*)

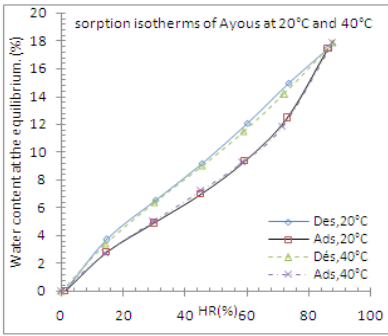


Figure 10. Sorption isotherms of ayous (*Triplochiton scleroxylon*)

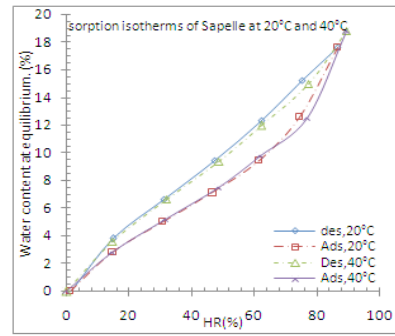


Figure 11. Sorption isotherms of sapele (*Entandrophragma cylindricum*)

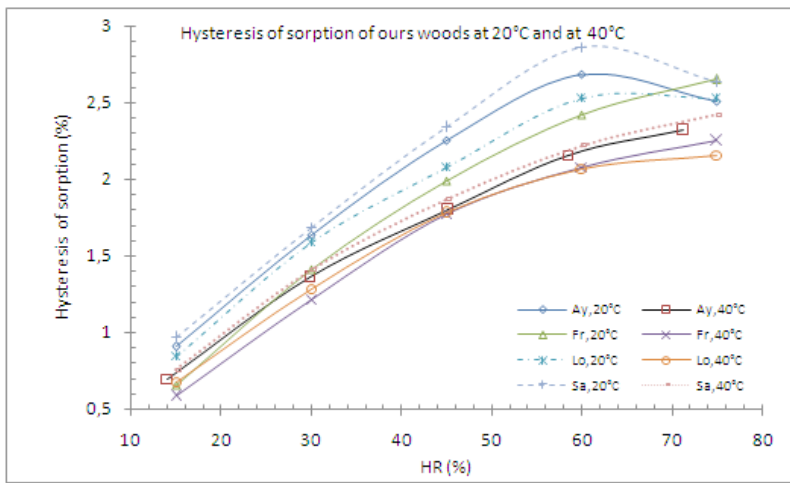


Figure 12. Hysteresis of sorption of our woods. Ay :ayous (*Triplochiton scleroxylon*) ; Fr :frake (*Terminalia superba*) ; Lo :lotofa (*Sterculia rhinopetala*) ; Sa :sapele (*Entandrophragma cylindricum*).

Tables 2 and 3 present the identified parameters of HH model of our wood specimen respectively at 20°C and 40°C. The curves and the experimental points are in the close agreement. The HH model seems to explain plausibly the sorption isotherms. The correlation coefficients (R^2) are close to 1 for all the fitted curves. Figure 13 shows experimental and predicted adsorption and desorption isotherms applied on sapele at 40°C and lotofa at 20°C.

Table 2. Identified parameters for sorption curves at 20°C and intensity of correlation (R^2).

| Wood species | HH model | | | | | | | |
|--|------------|--------|--------|-------|------------|-------|-------|-------|
| | Adsorption | | | | Desorption | | | |
| | A | B | C | R^2 | A | B | C | R^2 |
| Lotofa (<i>Sterculia rhinopetala</i>) | 5,302 | 8,405 | 9,878 | 0,998 | 4,094 | 4,259 | 3,621 | 0,933 |
| Frake (<i>Terminalia superba</i>) | 4,601 | 11,650 | 12,830 | 0,990 | 4,068 | 5,354 | 5,100 | 0,946 |
| Sapele (<i>Entandrophragma cylindricum</i>) | 3,613 | 12,000 | 12,080 | 0,995 | 3,140 | 6,068 | 4,750 | 0,972 |
| Ayous (<i>Triplochiton scleroxylon</i>) | 3,929 | 10,420 | 10,740 | 0,999 | 3,352 | 5,115 | 3,912 | 0,957 |

Table 3. Identified parameters for sorption curves at 40°C and intensity of correlation (R^2).

| Wood species | HH model | | | | | | | |
|--|------------|--------|--------|-------|------------|-------|-------|-------|
| | Adsorption | | | | Desorption | | | |
| | A | B | C | R^2 | A | B | C | R^2 |
| Lotofa (<i>Sterculia rhinopetala</i>) | 4,447 | 9,000 | 9,484 | 0,981 | 3,764 | 5,158 | 4,307 | 0,997 |
| Frake (<i>Terminalia superba</i>) | 4,028 | 12,420 | 12,600 | 0,935 | 3,679 | 7,152 | 6,489 | 0,980 |
| Sapele (<i>Entandrophragma cylindricum</i>) | 3,646 | 11,190 | 10,940 | 0,939 | 3,188 | 6,805 | 5,641 | 0,992 |
| Ayous (<i>Triplochiton scleroxylon</i>) | 4,034 | 9,280 | 9,319 | 0,981 | 3,554 | 5,028 | 4,006 | 0,995 |

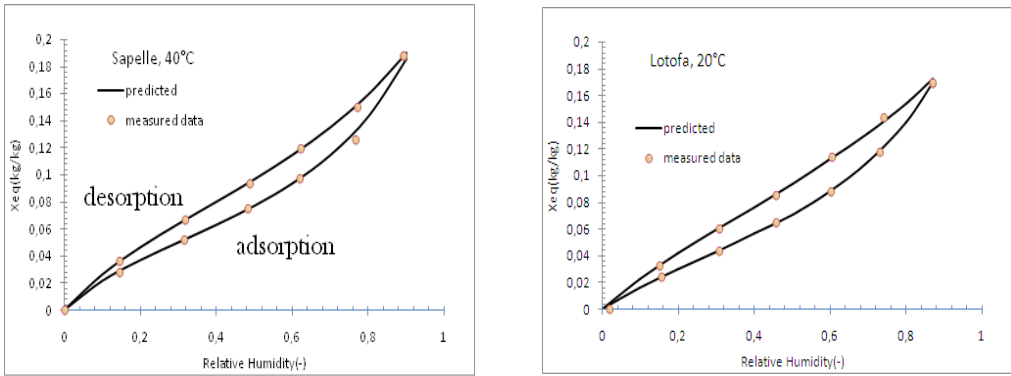


Figure 13. Comparison between adsorption and desorption envelope curves simulated by HH model and measured data for lotofa (*Sterculia rhinopetala*) at 20°C and sapele (*Entandrophragma cylindricum*) at 40°C.

Mass coefficient diffusion and Gas permeability

Figures 14 through 17 show the evolution of mass loss over time of each species when NaCl is used. We have obtained that the mass loss linearly increases with the time and it is in agreement with the results obtained by Agoua *et al.* (2001), Mouchot *et al.* (2006), Redman *et al.* (2012) and Rousset *et al.* (2004). We point out that for each species; two repetitions per sample were made. Each curve of these Figures (Figure 14-17) and Figure 18 corresponds to an independent experiment. As can be seen, only Figure 16 and 17 on lotofa and sapele woods respectively present a low variation of the slope. Note that for each species, all the samples are cut from the same longitudinal generatrix. Despite this care to limit the effect of wood variability the boards of ayous (Figure 14) and frake (Figure 15) may have mixed the sawing pattern along the board length. Therefore, the characterized transverse direction may have changed between the repetitions.

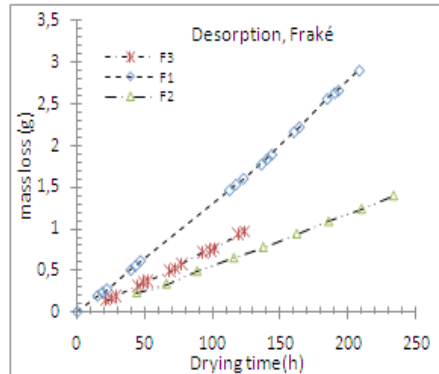
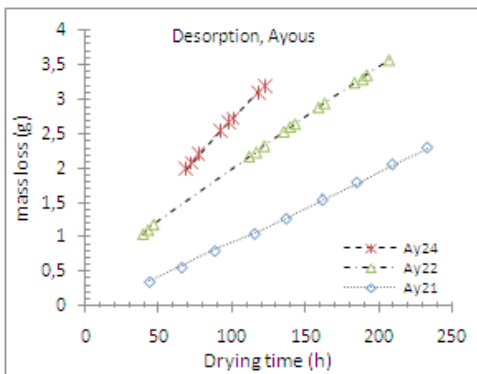


Figure 14. Mass loss versus time (NaCl, ayous). **Figure 15.** Mass loss versus time (NaCl, frake).

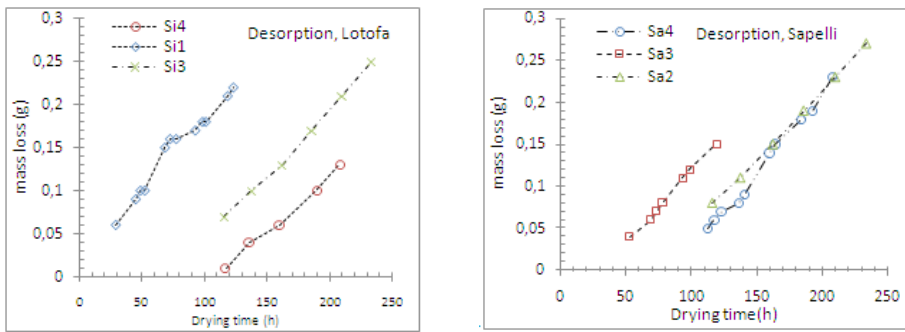


Figure 16. Mass loss versus time (NaCl, lotofa) **Figure 17.** Mass loss versus time (NaCl, sapele)

Figure 18 presents the evolution of gain mass versus the time when silica gel is used. We can notice that, the vapor flux is low in the case of lotofa and sapele (higher density) and high in the case of frake and ayous (lower density). Table 4 presents the measured diffusion coefficients of specimens tested. It is clear that the mass diffusivities are greater when it was measured with the “wet cup” (at higher moisture content) than with the dry cup (at lower moisture content). When NaCl is used, ayous gives the highest mass diffusivity coefficients in the order of 10^{-10} m²/s and the least is lotofa in the order of 10^{-11} m²/s. When silica gel is used, mass diffusivity coefficients of all studied species are in the order 10^{-11} m²/s. The mass diffusivities through lotofa and sapele are very close and markedly lower than the ayous and frake samples. The last species should have a relatively high drying rate.

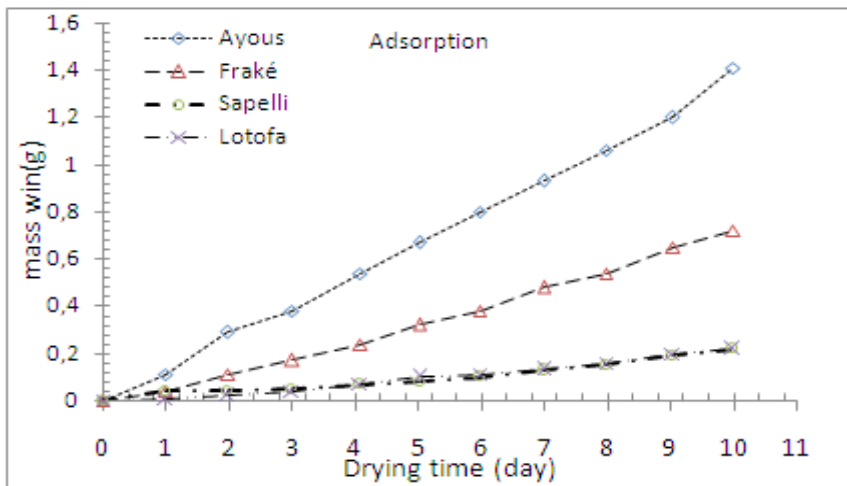


Figure 18. Evolution of gain mass with time using silica gel

The $f_{corrected}$ values for studied woods are presented in Table 4. In desorption, the obtained values on ayous and frake are expected range of $f_{corrected}$ for temperate woods (from 10^{-2} to 10^{-1} (Agoua 2001)). We report however that the values of the standard deviations are quite compatible with the values reported in the literature using the experimental device of the vaporimeter (Agoua 2001, Kouchade 2004, Mouchot *et al.* 2006). For example, the results obtained by Kouchade (2004) are presented in

Table 5. Such as Kouchade (2004), we observed that the samples taken side by side can present a great variety on their values of thermophysical properties. Effectively, heterogeneity of each species in the same log and between different logs of the same species causes the variations of obtained values.

Table 4. Mass diffusivity (using cutting method in steady state) and air permeability.

| Code number | $f_{corrected}$ ($\times 10^{-3}$) | Mass diffusivity (m^2/s) | | $\frac{\mu eP}{PSK}$ ($\times 10^9 mba.s.m^{-3}$) | Air permeability (m^2) | |
|--------------------------|---|-------------------------------------|-----------------------------|--|--|-----------------------------|
| | | Mean value ($\times 10^{-10}$) | SD ($\times 10^{-10}$) | | K, Mean value ($\times 10^{-18}$) | SD ($\times 10^{-18}$) |
| Sa2 (SS) ⁺ | 9,603 | 0,79 | 0,05 | 9,521 | 38,00 | 26,95 |
| Sa3 (SS) ⁺ | 10,173 | | | 45,72 | | |
| Sa4 (SS) ⁺ | 10,885 | | | 19,02 | | |
| Sa4 (Sili) [*] | 1,325 | 0,11 | -- | | | |
| Si1 (SS) ⁺ | 9,861 | 0,62 | 0,09 | 13,88 | 42,21 | 6,06 |
| Si3 (SS) ⁺ | 8,234 | | | 13,56 | | |
| Si4 (SS) ⁺ | 7,424 | | | 18,65 | | |
| Si2 (Sili) [*] | 1,480 | 0,11 | -- | 15,46 | | |
| Ay21 (SS) ⁺ | 69,232 | 9,63 | 5,00 | 29,93 | 36,10 | 47,58 |
| Ay22 (SS) ⁺ | 113,043 | | | 55,54 | | |
| Ay24 (SS) ⁺ | 198,990 | | | 6,024 | | |
| Ay23 (Sili) [*] | 9,075 | 0,69 | -- | 12,16 | | |
| F1 (SS) ⁺ | 90,066 | 4,70 | 2,10 | 4,26 | 79,76 | 60,46 |
| F2 (SS) ⁺ | 38,847 | | | 5,797 | | |
| F3 (SS) ⁺ | 50,826 | | | 12,26 | | |
| F4 (Sili) [*] | 4,705 | 0,37 | -- | 39,19 | | |

SS : NaCl ; Sili : Silica gel ; Sa : sapele ; Si : lotofa ; Ay : ayous ; F : frake. Adsorption(*) ; Desorption(+).SD: Standard deviation

Table 5. Published mass diffusivity of tropical woods in the tangential (T) and radial (R) directions using indirect method from electrical resistance measurement in unsteady state with thickness equal to 5mm (Kouchade 2004).

| Species | origin | Mass diffusivity (m^2/s) | | | |
|-------------------------------------|---------------|------------------------------|------------------------|------------------------|------------------------|
| | | Desorption | | Adsorption | |
| | | R($\times 10^{-10}$) | T($\times 10^{-10}$) | R($\times 10^{-10}$) | T($\times 10^{-10}$) |
| <i>Triplochiton scleroxylon</i> | Beninese wood | 4,03(0,88) | 3,52(1,56) | 3,40(0,58) | 3,32(0,43) |
| <i>Pelthogyne spp</i> | Latin America | 3,39(0,26) | 1,24(0,44) | 2,26(0,67) | 0,91(0,27) |
| <i>Afzelia africana</i> | Beninese wood | 3,30(1,69) | 1,19(0,13) | 2,16(1,39) | 1,12(0,35) |
| <i>Tabebuia spp</i> | Latin America | 1,41(0,33) | 0,69(0,06) | 0,64(0,17) | 0,40(0,11) |
| <i>Disternonanthus benthamianus</i> | Beninese wood | 3,56(0,79) | 1,23(0,17) | 2,43(0,47) | 1,02(0,18) |
| <i>Couratari spp</i> | Latin America | 5,56(0,52) | 1,49(0,11) | 5,40(0,64) | 1,33(0,11) |

Values in the brackets represent the standard deviations.

Figure 19 shows that mass diffusivity of our woods decreases exponentially when basal density of wood increases. Basal densities used are taken from Simo (2014). In the same experimental condition (steady state), this relationship is an advantage to estimate the value of unknown mass diffusivity of wood when their basal density is given.

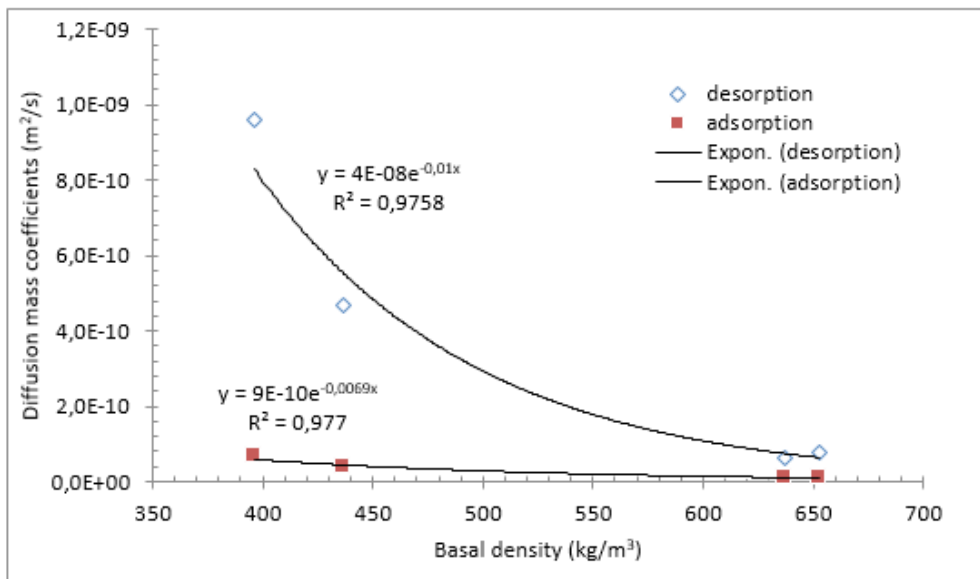


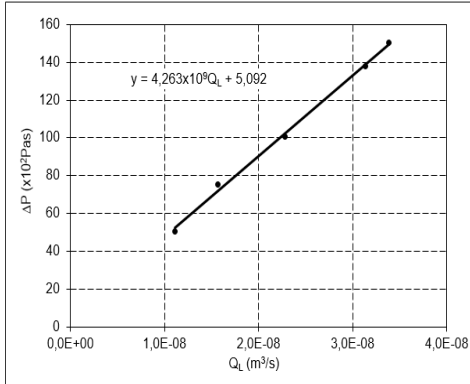
Figure 19. Evolution of mass coefficient diffusion with the basal density.

The list of values depicted in Table 6 gives the mass diffusivity and the air permeability measured on Australian hardwood samples by Redman *et al.* (2012) and on temperate samples by Agoua and Perré (2010). The authors of these results don't specify the part of the sample in the log (heartwood or sapwood). We can notice that our species are most permeable than those of Australian woods and less than those of temperate woods. Concerning the mass diffusivity, the obtained values with our tested species are higher than those of Australian woods. Sapele and lotofa have mass diffusivities lower than those of temperate woods, on the contrary to ayous and frake woods.

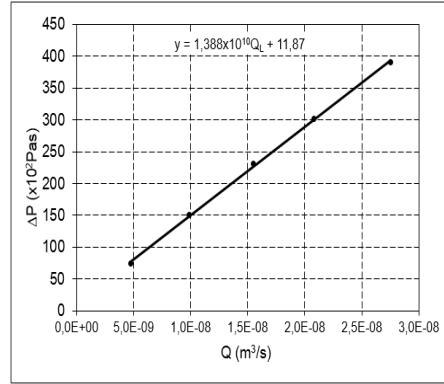
Table 6. Published mass diffusivity and permeability in the tangential (T) and radial (R) directions using cutting method in steady state with thickness equal to 13mm.

| Species | Mass diffusivity (m ² /s) | | Permeability (m ²) | | References |
|-----------------------------|--------------------------------------|------------------------|--------------------------------|------------------------|-----------------------------|
| | R(x10 ⁻¹⁰) | T(x10 ⁻¹⁰) | R(x10 ⁻¹⁸) | T(x10 ⁻¹⁸) | |
| <i>Corymbia citriodora</i> | 0,1 | 0,1 | -- | 0,003 | Redman <i>et al.</i> (2012) |
| <i>Eucalyptus pilularis</i> | 0,3 | 0,2 | 0,01 | 0,02 | Redman <i>et al.</i> (2012) |
| <i>Eucalyptus marginata</i> | 0,3 | 0,4 | 0,05 | 0,04 | Redman <i>et al.</i> (2012) |
| <i>Eucalyptus obliqua</i> | 0,7 | 0,4 | 8,6 | 0,30 | Redman <i>et al.</i> (2012) |
| <i>Pinus pinaster</i> | 4,3 | 2,9 | 1650 | 542 | Agoua and Perré (2010) |
| <i>Picea abies</i> | 1,6 | 1,3 | 110 | 516 | Agoua and Perré (2010) |
| <i>Fagus sylvatica</i> | 4,8 | 2,1 | 74 | 367 | Agoua and Perré (2010) |
| <i>Tectona grandis</i> | 2,8 | 1,7 | 4,82 | 5,69 | Agoua and Perré (2010) |

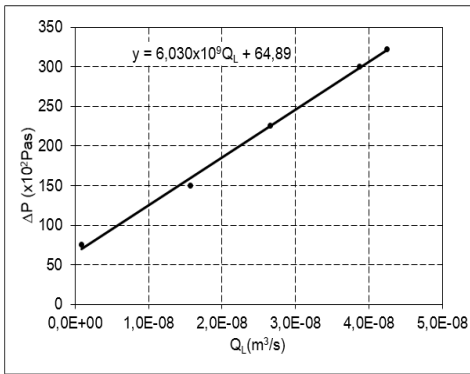
Concerning the air permeability, we plotted in Figure 20 the results for the samples F1, Si1, Ay24, Sa4 and we see that the relation (5) is quite well verified. Similar results are obtained for all samples and it is in agreement with the results obtained by Redman *et al.* (2012). We can notice here that it is difficult to find a relationship between the air permeability and the density (or mass diffusivity). The permeability of fraike is higher than the three others species. The obtained air permeability and standard deviations are compatible with those presented by Agoua (2001). The observed differences are probably due to the heterogeneity of the samples taken along the same board.



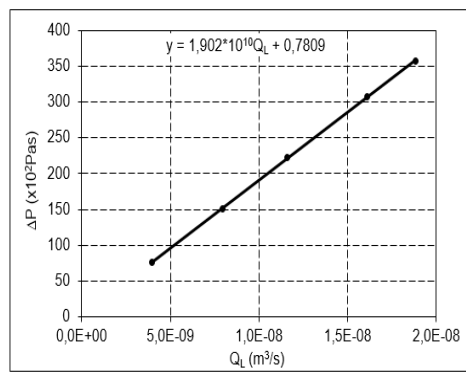
Fraike (*Terminalia superba*) : F1



Lotofa (*Sterculia rhinopetala*) : Si1



Ayous (*Triplochiton scleroxylon*): Ay24



Sapele (*Entandrophragma cylindricum*) : Sa4

Figure 20. ΔP versus QL of selected wood samples.

Previous studies on the effect of vessel properties on permeability reported the positive effect of vessel size and frequency, the great negative effect of vessel with tyloses on permeability in different species (Booker 1977, Taghiyari *et al.* 2014). Thus along studied direction, the size and frequency of vessel are probably higher on frake than the others studied wood or/and frake has less tyloses along vessel than the others. According to Taghiyari *et al.* (2014), the parts of log (heartwood and sapwood) also influence the obtained results.

CONCLUSIONS

Characterization of sorption isotherm, mass diffusivity (in the steady state) and air permeability were achieved for four Central Africa tropical woods. Results on studied woods show that:

Relative humidity most affects equilibrium states than temperature and the increasing of temperature reduced the magnitude of hysteresis of sorption.

At a given temperature, Hailwood-Horrobin model's (1946) can be used to describe nicely their sorption isotherms, as well as adsorption than desorption. The model parameters are given for the four species of this work.

The air permeability was in the order 10^{-17}m^2 . These values are compared to those obtained in the literature for some Australian hardwoods and for some temperate woods.

It is difficult to find a comprehensive relation between the air permeability, the density and the mass diffusivity.

In desorption phase, the mass diffusivity was in the order $10^{-11} \text{m}^2/\text{s}$ for sapele and lotofa and in the order $10^{-10} \text{m}^2/\text{s}$ for frake and ayous.

In adsorption phase, the mass diffusivities were lower than those obtained in desorption phase and for all studied woods, these mass diffusivities was in the order $10^{-11} \text{m}^2/\text{s}$.

Comparing to the temperate woods, the low diffusion coefficient of Central Africa woods like sapele and lotofa implied a slow drying rate.

The obtained air permeability and mass diffusivity on the samples taken along the same board present some differences probably due to the heterogeneity of each species.

The mass diffusivity is well correlated with the basal density by an exponential function.

The results obtained in this study have provided valuable information on the mass transfer properties of some Central Africa woods. These values can be used to promote the use of these woods and to improve their drying process with a comprehensive drying model.

Some further works have to be performed to complete this study: (i) Extend the sampling to different trees to appreciate more correctly the variability of these parameters, (ii) The sawing pattern of the samples have to be made with the greatest care for characterizing the mass transfer properties according to the different material directions, (iii) For the mass diffusivities, it is also necessary to plan some measurements in variable wood moisture range in order to specify the possible variation of the diffusivities versus wood moisture.

ACKNOWLEDGMENTS

The principal author would like to thank Mr. Tristan Stein for the sampling collection of our woods and the setting of apparatus measures. This same author acknowledges the International Tropical Timber Organization (ITTO) who financed a part of this work (ITTO Ref. Number: 011/11A).

REFERENCES

- Agoua, E. 2001.** Diffusivité et perméabilité du bois: Validation de méthodologies expérimentales et prise en compte de paramètres morphologiques simples pour la modélisation physique. Thesis, EN-GREF, Nancy, France.
- Agoua, E.; Perré, P. 2010.** Mass transfer in wood: Identification of structural parameters from diffusivity and permeability measurements. *Journal of Porous Media* 13(11): 1017-1024.
- Agoua, E.; Zohoun, S.; Perré, P. 2001.** A double climatic chamber used to measure the diffusion coefficient of water in wood in unsteady-state conditions: determination of the best fitting method by numerical simulation. *International Journal of Heat and Mass Transfer* 44: 3731-3744.
- Alix, S.; Philippe, E.; Bessadok, A.; Lebrun L.; Morvan, C.; Marais, S. 2009.** Effect of chemical treatments on water sorption and mechanical properties of flax fibres. *Bioresource Technology* (100): 4742-4749.
- ATIBT (la lettre de l'ATIBT). 2002.** Commerce mondial des bois tropicaux : entre demande asiatique et pression écologiste occidentale. n° 16, été 2002.
- Beguide, B.; Simo, T.M. 2005.** Une contribution à l'étude du séchage du bois d'ayous et de l'ébène. *Phys Chem News* 26: 52-56.
- Benoit, Y. 2008.** Le guide des essences bois : 74 essences, les choisir, les reconnaître, les utiliser. 2^{ème} édition, FCBA, Eyrolles.
- Björk, H.; Rasmuson, A. 1995.** Moisture equilibrium of wood and bark chips in superheated steam. *Fuel* 74 (12): 1887-1890.
- Booker, R.E. 1977.** Problems in the measurement of longitudinal sapwood permeability and hydraulic conductivity. *New Zealand Journal of Forestry Science* 7(3): 297-306.
- Comstock, G. L.; Côté W.A. JR. 1968.** Factors affecting permeability and pit aspiration in coniferous sapwood. *Wood Science and Technology* 2: 279-291.
- Engelund, E. T.; Klamer, M.; Venås, T.M. 2010.** Acquisition of sorption isotherms for modified woods by the use of dynamic vapour sorption instrumentation. Principles and Practice. Paper prepared for the 41st Annual Meeting, Biarritz, France, 9-13 May 2010, IRG/WP 10-40518.
- Fernández, F.G.; Esteban, L.G.; De Palacios, P.; Simon, C.; Iruela, A.G.; De la Fuente, J. 2014.** Sorption and thermodynamic properties of *Terminalia superb* Engl. & Diels and *Triplochiton scleroxylon* K. Schum. through the 15, 35 and 50°C sorption isotherms. *Eur J Wood Prod* 72:99-106.
- Gholamiyan, H.; Tarmian, A.; Hosseini, K.D.; Azadfallah, M. 2012.** The potential use of organosilane water soluble nanomaterials as water vapor diffusion retarders for wood. *Maderas. Ciencia y tecnología* 14(1): 43-52.

Hailwood A.J.; Horrobin S. 1946. Absorption of water by polymers: analysis in terms of a simple model. *Trans Faraday Soc* 42B: 84-102.

Hill, C.A.S.; Norton, A.J.; Newman, G. 2009. The Water vapor sorption behavior of natural fibers. *Journal of Applied Polymer Science* (112): 1524-1537.

Jalaludin, Z.; Hill, C.; Kermani, A. 2009. Moisture adsorption isotherms of wood using dynamic vapor sorption. CTE, SEBE, Napier University, Edinburgh, UK.

Jannot, Y. 2008. Isothermes de sorption: modèles et détermination. 16pages.

Jannot, Y.; Kanmogne, A; Talla, A.; Monkam, L. 2006. Experimental Determination and Modelling of Water Desorption Isotherms of Tropical Woods: Afzelia, Ebony, Iroko, Moabi and Obeche. *Holz als Roh-und Werkstoff* 64(2): 121 - 124.

Kouchade, A.C.2004. Détermination en routine de la diffusivité massique dans le bois par la méthode inverse à partir de la mesure électrique en régime transitoire. Ph.D. Thesis, ENGREF, France.

Mantanis, G.I.; Papadopoulos, A.N. 2010. The sorption of water vapour of wood treated with a nanotechnology compound. *Wood Sci Technol* 44(3):515-522.

Mouchot, N. ; Thiercelin, F. ; Perre, P. ; Zoulalian, A. 2006. Characterization of diffusionnal transfers of bound water and water vapor in beech and spruce. *Maderas. Ciencia y tecnología* 8(3): 139-147.

Olek, W.; Majka, J.; Czajkowski, L. 2012. Sorption isotherms of thermally modified wood. *Holzforschung* :67(2): 183-191.

Pang, S. 2007. Mathematical modeling of kiln drying of softwood timber: model development, validation and practical application. *Drying technology* 25: 421-431.

Perré, P. 2004. Le séchage des matériaux déformables : formulation, caractérisation physico-mécanique, modélisation et simulation. *Transactions TSTU*, 10(1A):120-139.

Perré, P.; Turner, I.W. 1999. A 3-D version of TransPort: A comprehensive heat and mass transfer computational model for simulating the drying of porous media. *Int J of Heat and Mass Transfer* 42: 4501-4521.

Popper, R.; Niems, P.; Croptier, S. 2009. Adsorption and desorption measurements on selected exotic wood species. Analysis with the Hailwood-Horrobin model to describe the sorption hysteresis. *Wood Research* 54 (4): 43-56.

Redman, A.L.; Bailleres, H.; Turner, I; Perré, P. 2012. Mass transfer properties (permeability and mass diffusivity) of four Australian hardwood species. *BioResources* 7(3): 3410-3424.

Rousset, P.1999. Détermination des propriétés de diffusion, de sorption et de perméation du bois de peuplier traité à haute température en vue d'une utilisation comme emballage alimentaire. DEA Thesis, University of Montpellier 1, ENSAM, France.

Rousset, P.; Perré, P. ; Girard, P. 2004. Modification of mass transfer properties in poplar wood (*P. robusta*) by a thermal treatment at high temperature. *Holz als Roh- und Werkstoff* 62: 113-119.

Schmid, T.; Naderi, M. 2010. An introduction to DVS and IGC technologies. SWST conference, Geneva.

Simo, T.M. 2014. Experimental characterization of the influence of water content on the density and shrinkage of tropical woods coming from Cameroon and deduction of their fiber saturation points. *International Journal of Science and Research* 3(6): 510-515.

Simo, T.M.; Bonoma, B.; Njomo, D. 2010. Modélisation et simulation numérique du séchage des bois d'ayous et d'ébène. Validation expérimentale. *Revue des Energies Renouvelables* 13(1): 13-24.

Simo, T.M.; Bonoma, B.; Njomo, D. 2011. Modélisation du séchage convectif et symétrique des bois d'ayous, d'eucalyptus grandis et d'ébène. Simulation numérique et validation expérimentale. *Afrique Science* 7(3): 15-32.

Simpson, W.T. 1973. Predicting equilibrium moisture content of wood by mathematical models. *Wood Fiber* 5:41-49.

Simpson, W.T. 1980. Sorption theories applied to wood. *Wood and Fiber* 12(3): 183-195.

Surface Measurement Systems. 2015. DVS Intrinsic System Brochure, [online]<www.smsuk.co.uk, www.smsna.com> [available: 6/06/ 2015].

Taghiyari, H.R.; Oladi, R.; Miri-Tari, S.M.; Habibzade, S. 2014. Effects of diffusion drying schedules on gas and liquid permeability in *Paulownia fortunei* wood. *Bosque* 35(1): 101-110.

Tekleyohannes, A.T. 1995. Unified and heterogeneous modeling of water vapor sorption in Douglas-fir wood with artificial neural networks. Ph.D Thesis, University of British Columbia.

Time, B. 1998. Hygroscopic moisture content in wood. Doctor Engineer Thesis, Norwegian University of Sciences and Technology, 232p.

Turner, J.; Perré, P. 1995. A comparison of the drying simulation codes TransPore and Wood 2D which are used for the modeling of two-dimensional wood drying processes. *Drying Technology*. Special issue: *Mathematical Modelling and Numerical Techniques for the Solution of Drying Problems*. 13(3): 695-735.

Zohoun, S.; Agoua, E.; Degan, G.; Perré, P. 2003. An experimental correction proposed for an accurate determination of mass diffusivity of wood in steady regime. *Heat and Mass Transfer* 39: 147-155.